Quantum Computers and Cellular Phones

Robert Calderbank

Duke University and Cohere Technologies

Abstract: This talk will describe how the geometry of the Heisenberg-Weyl group provides a common foundation for quantum computing and wireless communication.

Disclosure: Advisor to IonQ

Part 1

The Heisenberg-Weyl group in the quantum world

Quantum Error Correction

Biased Noise

Coherent Noise and Decoherence-Free Subspaces

Biased Noise and Clifford Deformations

The Computer as a Physics Experiment

ENIAC (1945)

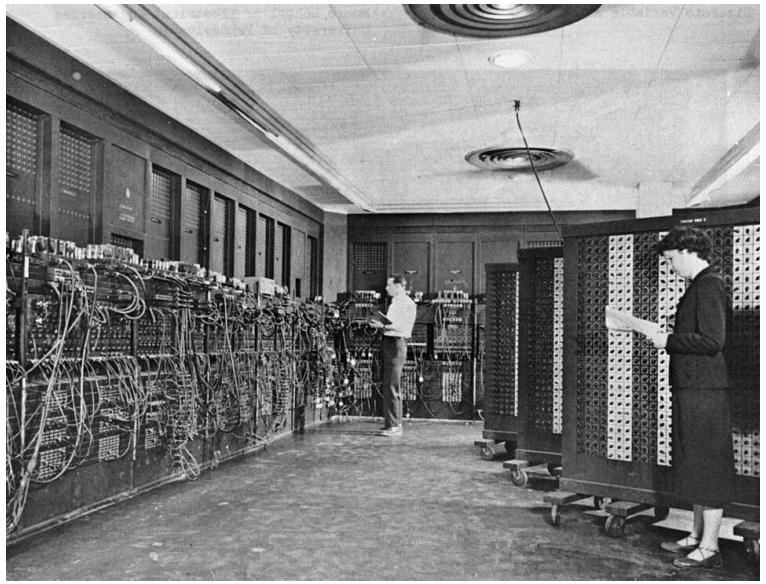

Neutral Atom Quantum Computer
QuERA (2023)

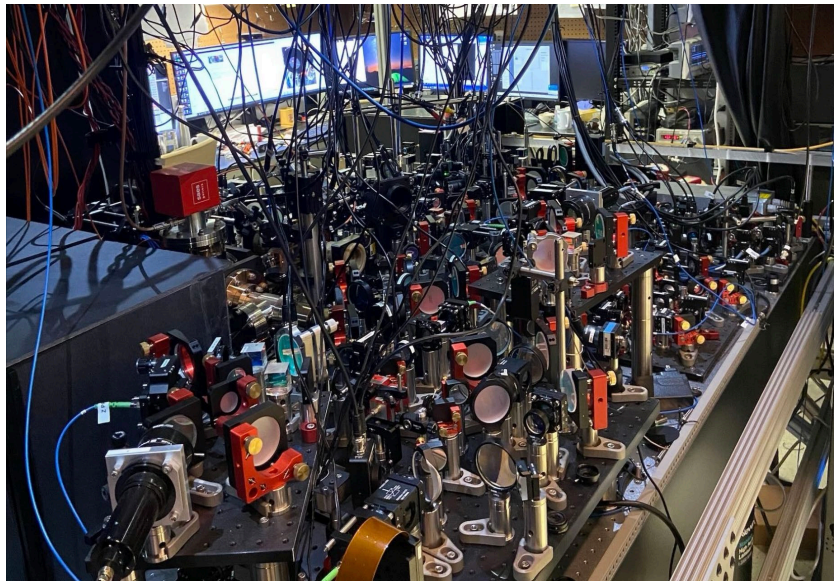

The Need for Quantum Error Correction

- Qubits are highly susceptible to errors resulting from imperfect control, unwanted interactions, and decoherence. This greatly limits the number of reliable logical qubits and logic operations in a quantum device.

- We can reduce logical error rates to be arbitrarily low with appropriate **quantum error correction (QEC)** protocols if the physical error rate is below a **threshold value**.

- Implementation of QEC requires additional spatial and temporal overhead.

E. Knill, R. Laflamme, and W. H. Zurek, **Resilient quantum computation**. Science 279, 342 (1998).

D. Aharonov, and B. Michael, **Fault-tolerant quantum computation with constant error,** Proceedings of the twenty-ninth annual ACM symposium on Theory of computing. (1997).

A. Kitaev, **Quantum error correction with imperfect gates,** Quantum communication, computing, and measurement. Boston, MA: Springer US, 181-188 (1997).

Quantum Bits

Classical Bit: takes the value 0 or the value 1

Quantum Bit: physical system that can take on a superposition of two base states 0 (e_0=(0,1)) and 1 (e_1=(1,0)) – a 2-dim complex Hilbert space $\mathbb{C}^2$

Given a real or complex vector of length $N=2^m$ order the coordinates from right to left, from 0 to $2^m - 1$, and label the i^{th} entry with the binary expansion of i

$$e_2 = e_{10} = (0100) = (10) \otimes (01) = e_1 \otimes e_0$$
$$e_6 = e_{110} = (01000000) = (10) \otimes (0100) = e_1 \otimes e_1 \otimes e_0$$

$\mathbb{C}^8 = \mathbb{C}^2 \otimes \mathbb{C}^2 \otimes \mathbb{C}^2$: If qubit i is in state v_i then the system is in state $v_1 \otimes v_2 \otimes v_3$

Resolution of the Identity: Operators P_i i=1, … ,t projecting onto spaces V_i i=1, … , t satisfying

$$P_i P_j = 0 \text{ if } i \neq j \text{ and } P_1 + ... + P_t = I$$

von Neumann Measurement (wrt P_i i=1, … ,t): A unit vector v projects onto V_i with probability $v P_i v^*$ and we learn the index I of the projection that occurs

Quantum Errors

Completely Depolarizing Channel:

$$X = E(1, 0) = \begin{pmatrix} 0 & 1 \\ 1 & 0 \end{pmatrix} \qquad Z = E(0, 1) = \begin{pmatrix} 1 & 0 \\ 0 & -1 \end{pmatrix} \qquad y = E(1, 1) = iXZ = \begin{pmatrix} 0 & -i \\ i & 0 \end{pmatrix}$$

Flip Error **Phase Error** **Flip - Phase Error**

Pauli Group P_3: given binary 3-tuples $a = (a_1, a_2, a_3)$ and $b = (b_1, b_2, b_3)$ define

$$E(a, b) = i^{(a,b)} \; X^{a_1} Z^{b_1} \otimes X^{a_2} Z^{b_2} \otimes X^{a_3} Z^{b_3}$$

$v = (v_1, v_2, v_3)$

$E(000, \mathbf{110}) =$ 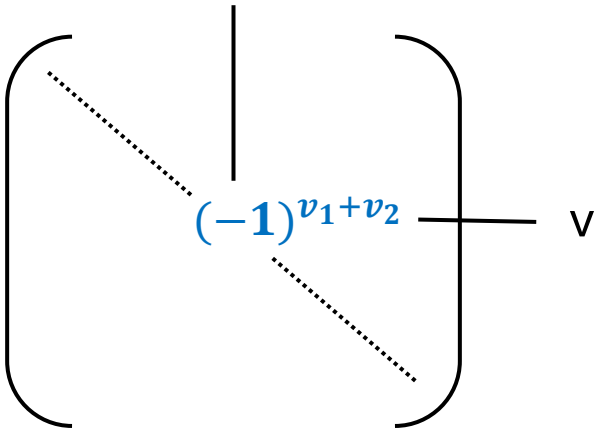

$v = (v_1, v_2, v_3)$

$E(000, \mathbf{011}) =$ 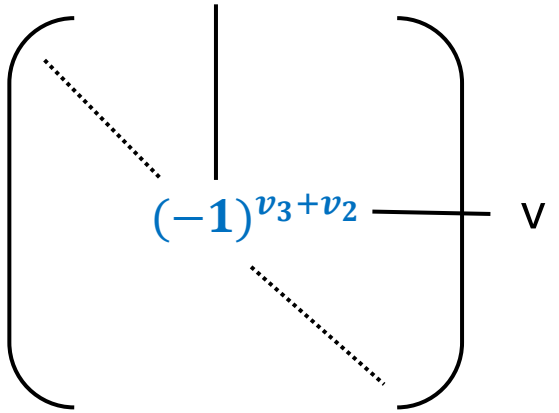

The Pauli Group and the Clifford Group

Pauli Group P_m: $\{\pm E(a, b), \pm i\, E(a, b)\}$

$$E(a, b)\, E(c, d) = \begin{cases} E(c, d)\, E(a, b), & \text{if } ad^T + bc^T = 0 \pmod 2 \\ -E(c, d)\, E(a, b), & \text{if } ad^T + bc^T = 1 \pmod 2 \end{cases}$$

Commutative subgroups correspond to isotropic subspaces

Clifford Group $Cliff_m$: The normalizer of the Pauli group in the full unitary group – $Cliff_m$ acts transitively on isotropic subspaces of a given dimension

If $g \in Cliff_m$ then $g^* E(a, b)\, g = \pm E[(a, b)F]$ where $F \Omega F^T = \Omega$ and $\Omega =$ $\begin{pmatrix} 0 & I_m \\ I_m & 0 \end{pmatrix}$

Examples: $\otimes_m H_2$ where H_2 is the 2x2 Walsh-Hadamard matrix

$\mathrm{diag}[i^{Q(v)}]$ where $Q(v)$ is a Z_4 valued quadratic form

Elements of $Cliff_m$ implement quantum gates

Quantum Errors Permute Eigenspaces

Stabilizer Group S: $< g_1 = E(000, 110), g_2 = E(000, 011) >$

Projection Matrix

$$P_{++} = [(I_8 + E(000, 110))/2]\,[(I_8 + E(000, 011))/2]$$

Conjugation: $P_{++} \rightarrow E(001, 000)^* P_{++} E(001, 000)$

$$P_{+-} = [(I_8 + E(000, 110))/2]\,[(I_8 - E(000, 011))/2]$$

Eigenspace

V_{++}

$V_{++} \rightarrow V_{+-} = V_{++} E(001, 000)$

V_{+-}

The resolution of the identity is preserved by every Pauli error

$V_{++} \longleftrightarrow V_{+-}$ $V_{-+} \longleftrightarrow V_{--}$ **$E(001, 000)$**

The Bit Flip Code

The bit flip code protects against a single flip error on 3 qubits

$V_{++} = < e_{000}, e_{111} >$: Start with a single protected qubit $v = \alpha\, e_{000} + \beta\, e_{111}$

There are 3 eigenspaces different from V_{++} and 3 single flip errors – different single flip errors take V_{++} to different eigenspaces

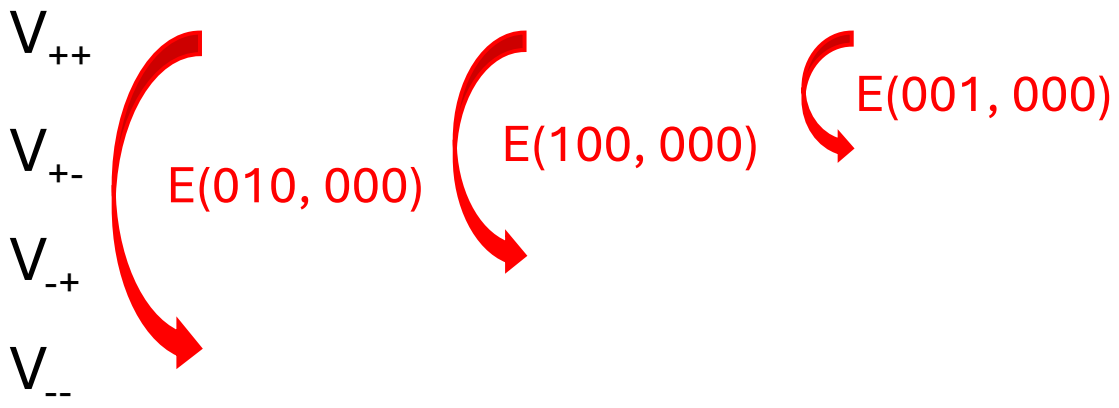

We identify the eigenspace without getting any information about α and β

There are other ways of transitioning from V_{++} to V_{--} (for example E(101, 000)) but the most probable is E(010,000)

Syndrome Decoding in the Quantum World: Stabilizer Codes

3 qubits: 8-dimensional Hilbert space $\mathbb{C}^8$

Error Model: Independent bit flips and phase flips

Error Group: Pauli group P_3 – all quantum errors on 3 qubits

Stabilizer Group: $S = \langle g_1, g_2 \rangle$ - 2-dim commutative subgroup of P_3 generated by g_1 and g_2

Bit Flip Code: $V_{++} = \{ v \in \mathbb{C}^8 \mid g_1 v = v,\ g_2 v = v \}$ – the fixed space of S

Resolution of the Identity: $\mathbb{C}^8 = V_{++} + V_{+-} + V_{-+} + V_{--}$ - the Pauli group permutes the spaces $V_{\varepsilon\delta}$

Quantum Channel: $v \in V_{++} \rightarrow g(v) \in V_{\varepsilon\delta}$

Syndrome Decoding: The stabilizers g_1, g_2 identify ε, δ

Decoder: Outputs e[g(v)] where e is the most probable error given that $g(v) \in V_{\varepsilon\delta}$

Biased Noise

Each quantum system has its own set of dominant errors.

- Erasure[1,2]
- Leakage[3]
- **Dephasing**[4,5]

[1] H. Aghaee Rad, et al, **Scaling and networking a modular photonic quantum computer,** *Nature* 638.8052 912-919 (2025).

[2] D. Bluvstein, et al. **A quantum processor based on coherent transport of entangled atom arrays,** *Nature* 604.7906 451-456 (2022).

[3] Google Quantum AI and Collaborators, **Quantum error correction below the surface code threshold,** *Nature* **638**, 920–926 (2025).

[4] C. Ballance, T. Harty, N. Linke, M. Sepiol, and D. Lucas, **High-fidelity quantum logic gates using trapped-ion hyperfine qubits**, Phys. Rev. Lett. 117, 060504 (2016).

[5] P. Aliferis, F. Brito, D. P. DiVincenzo, J. Preskill, M. Steffen, and B. M. Terhal, **Fault-tolerant computing with biased-noise superconducting qubits: a case study**, New J. of Physics. 11, 013061 (2009).

Biased Noise Model

Consider a code capacity noise model with the following single-qubit depolarizing noise channel:

$$\mathcal{E}[\rho] = (1-p)\rho + p_x X\rho X + p_y Y\rho Y + p_z Z\rho Z$$

$\mathbf{p}$ is the total physical error rate such that $\boldsymbol{p = p_x + p_y + p_z}$

The parameter quantifying the bias is $\boldsymbol{\eta = \frac{p_z}{p_x + p_y}}$

For simplicity, we assume $\boldsymbol{p_x = p_y}$

$\boldsymbol{\eta = 0.5}$ corresponds to the standard depolarizing error channel, where all Pauli errors occur with the same probability. There is no bias toward any single Pauli error.

Coherent Noise

Physical platforms such as trapped ions suffer from coherent noise where errors accumulate in a particular direction and can be more damaging.

Development of quantum error correcting codes that are oblivious to coherent noise removes a physical roadblock to fault tolerant quantum computation.

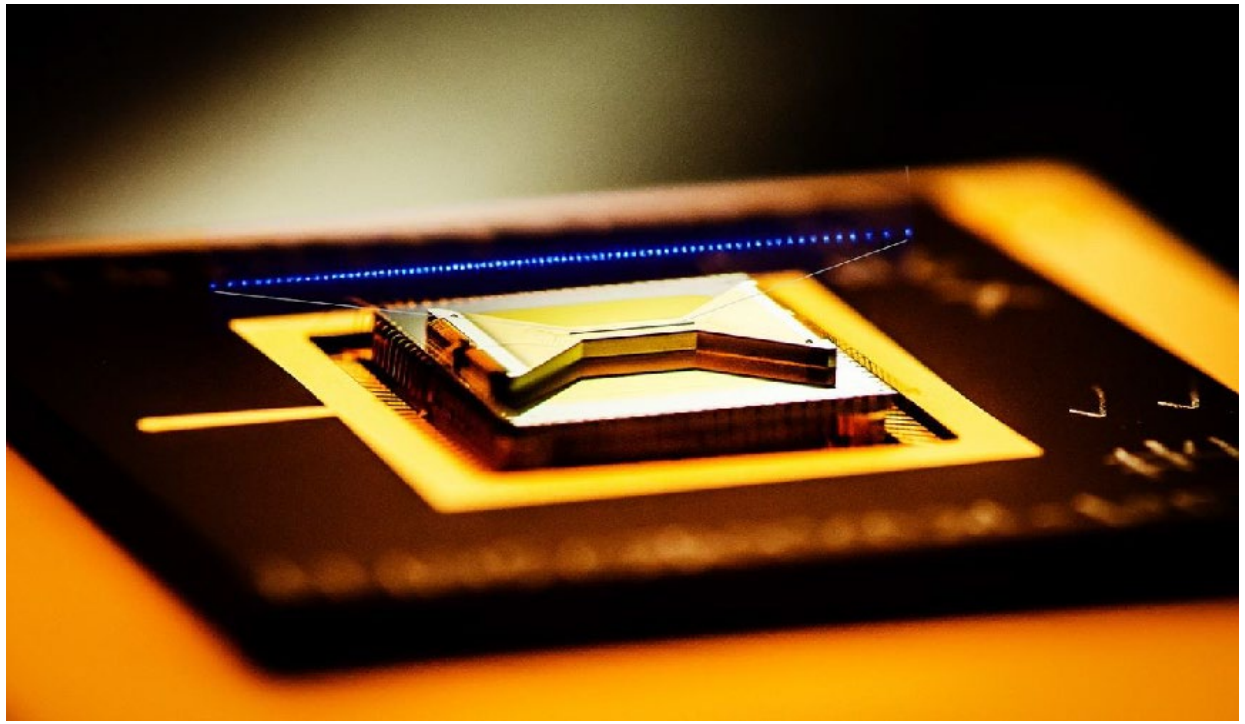

Ion trap fabricated by Sandia National Laboratories and used by experimental teams at Duke and IonQ

J. Hu, Q. Liang, N. Rengaswamy, R. Calderbank, **Mitigating coherent noise by balancing weight 2 Z-stabilizers**, *IEEE Transactions on Information Theory, vol. 68, no. 3, pp. 1795-1808, March 2022*

Quantum Codes that are Oblivious to Coherent Noise

Coherent noise acts transversally giving rise to an effective error, which is a (unitary) Z-rotation on each qubit by some (small) angle θ.

Rather than address coherent noise through active error correction, we investigate passive mitigation through decoherence free subspaces.

We require the noise to preserve the code space, and to act trivially (as the logical identity operator) on the protected information. Thus, we develop conditions for all transversal Z-rotations to preserve the code space of a stabilizer code.

CSS Codes: Stabilizer group generated by pure X-type errors and pure Z-type errors

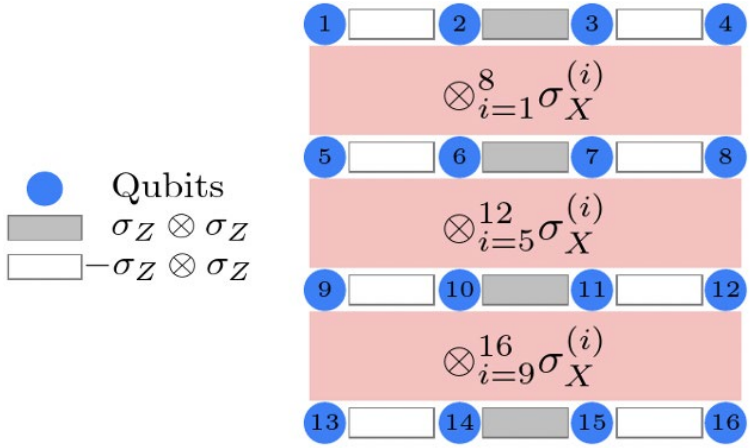

[[$4L^2$, 1, L]] Shor Code: Concatenation of the [[4; 1]] bit-flip code and the [[4; 1]] phase-flip code

Clifford Deformations

XZZX deformation = a Hadamard transformation on every other qubit.

$$HXH = Z$$
$$HZH = X$$

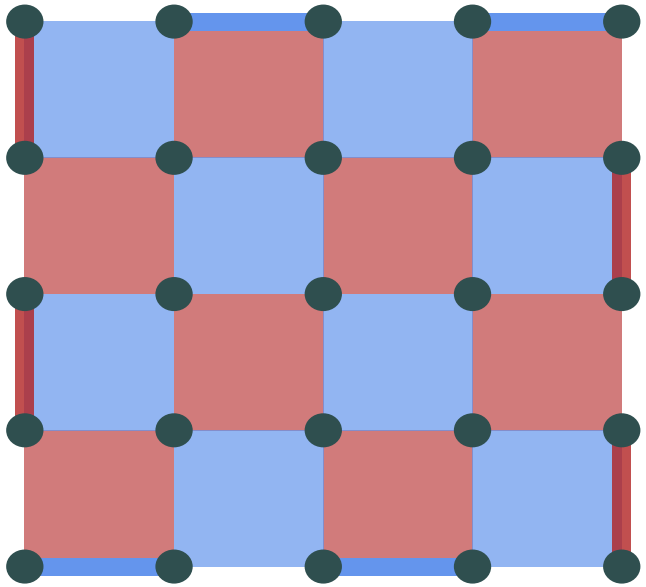

The **Clifford deformation**[1] of a stabilizer code is the application of Clifford transformations to the code space, modifying the stabilizers.

An example of Clifford deformed surface codes is the **XZZX surface code**[2] which has high thresholds in the presence of biased noise models

[1] A. Dua, et al. **Clifford-deformed surface codes,** PRX Quantum, 5(1), 010347 (2024).

[2] J . P. Bonilla Ataides, et al. **The xzzx surface code**, Nature (London) 12, 2172 (2021).

Co-design of CSS Codes and Clifford Deformations

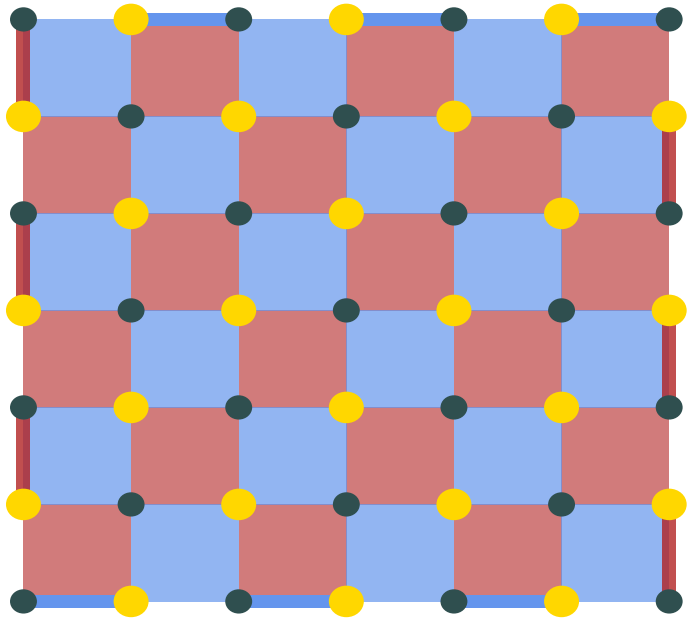

Elongated Compass Codes: More stabilizers gathering information on the dominant errors

XZZX-Deformed Compass Codes: Hadamard transformation on the upper right and lower left qubits supporting weight-4 X stabilizers ("square" stabilizers) – aligns code space with the noise

Combining the two ideas improves performance.

J. A. Campos and K. R. Brown**, Clifford-deformed compass codes,** arXiv preprint arXiv: 2412.03808 (2024).

Part 2

The Heisenberg-Weyl group in the wireless world

A Pulse in the Delay-Doppler Domain

Pulses as Geometric Modes

Symplectic Transformations

Insights from 1954

George Orwell: *Every generation imagines itself to be more intelligent than the one that went before it, and wiser than the one that comes after it.*

2G
TDMA

Voice

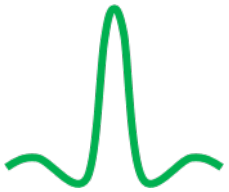

Localization in Time

3G
CDMA

Voice +Data

Localization in Code

4G
OFDM

High Speed Data

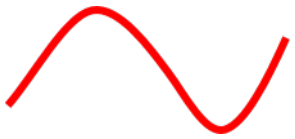

Localization in Frequency

5G & Beyond
OTFS

Massive IoT
Extreme Mobility
Extreme Broadband

Localization in Delay / Doppler

Localization in Delay and Doppler

Radar as a game of 20 questions with an operator

P.M. Woodward: *Probability and Information Theory, with Applications to Radar,* Pergamon Press, 1953

He viewed the problem of localizing a scatterer in delay and Doppler as using a waveform to ask questions of the operator defined by the radar scene

How to Design a Question:

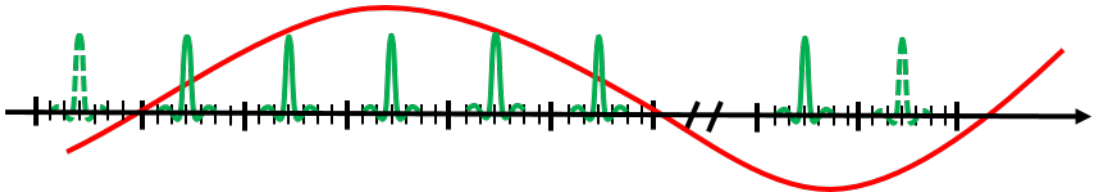

Channel prediction as a game of 20 questions with a wireless channel

Imagine a Pulse in the DD Domain

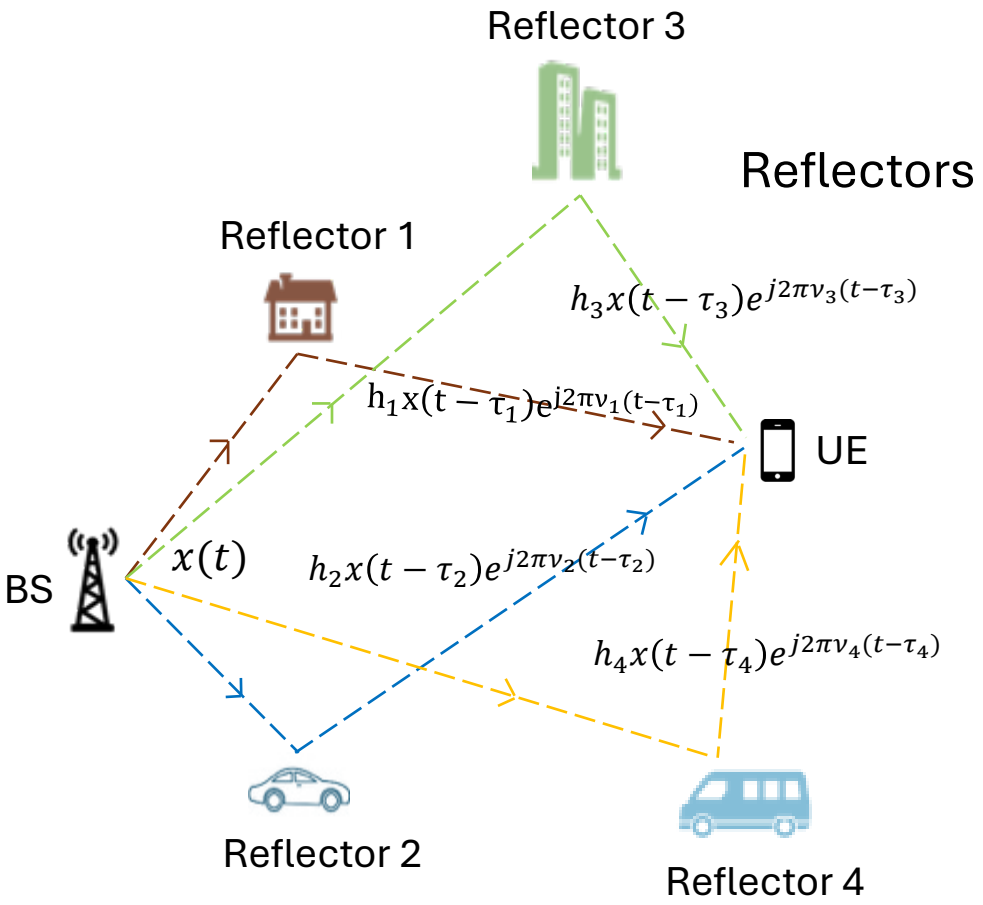

Manifest as Taps in Delay and Doppler

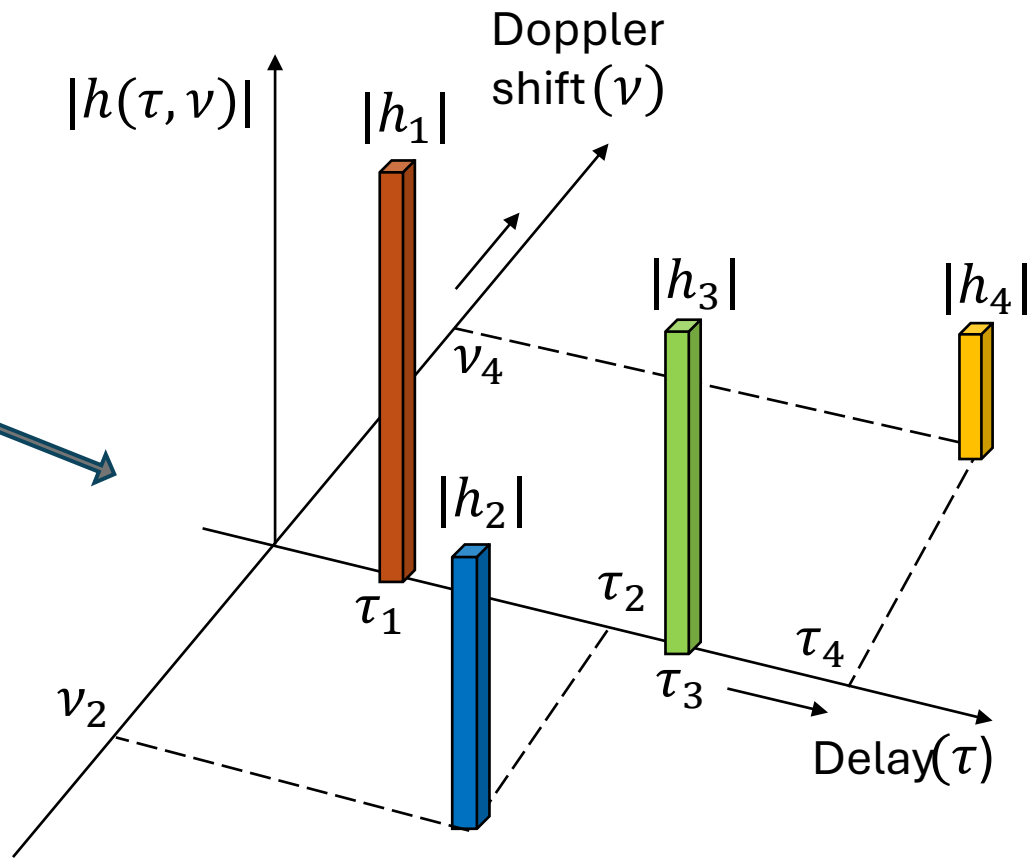

A pulse in the DD domain is an ideal radar waveform

A Pulse in the Delay-Doppler Domain

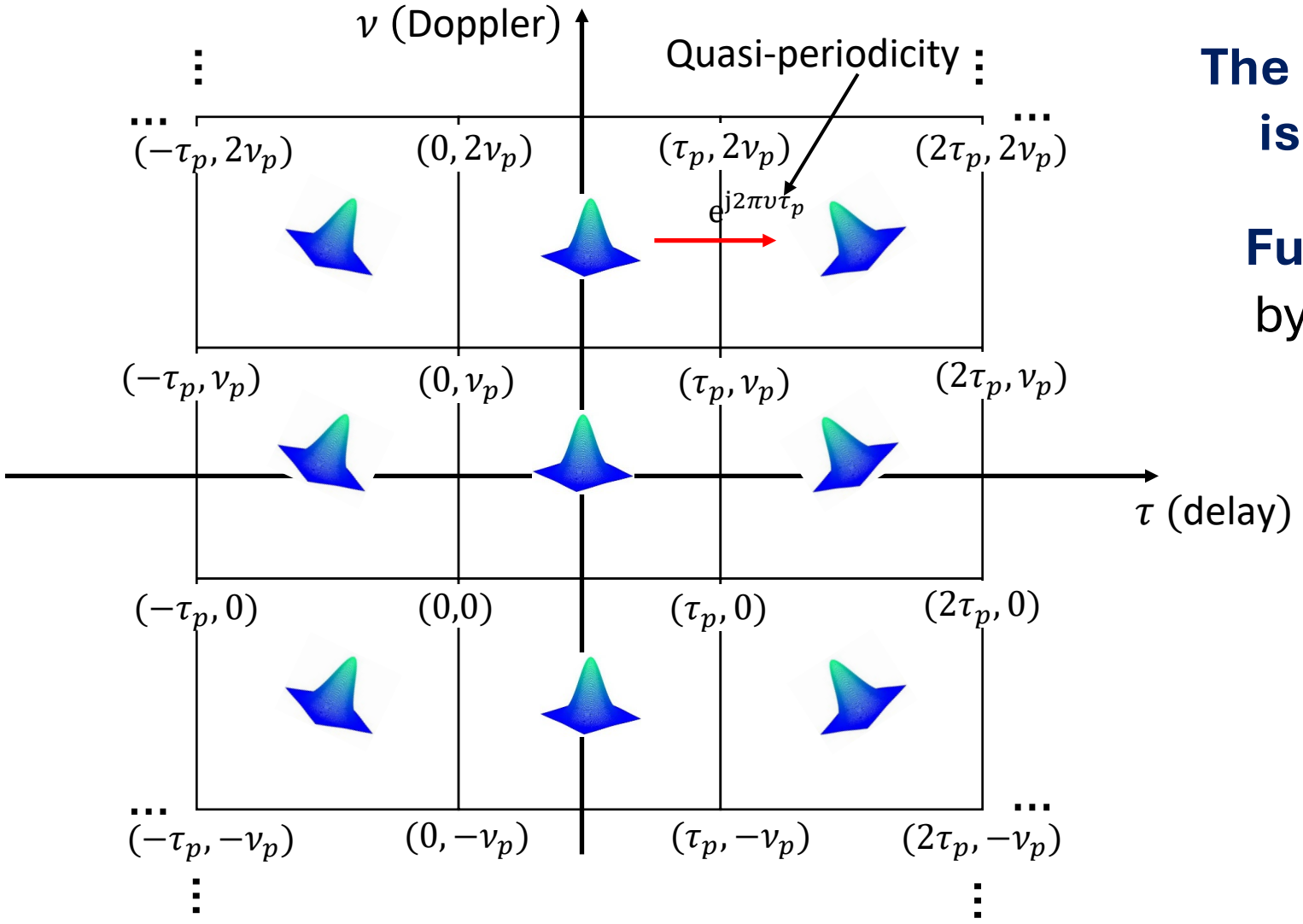

The DD realization of a TD signal is a quasi-periodic function

Fundamental Domain defined by the delay period τ_p and the Doppler period $\nu_p = 1/\tau_p$

Delay Spread

ν_p= 20 KHz

Doppler Spread

τ_p= 50 μs

TD Pulsone from a Quasi-Periodic DD Domain Pulse

TD Pulsone

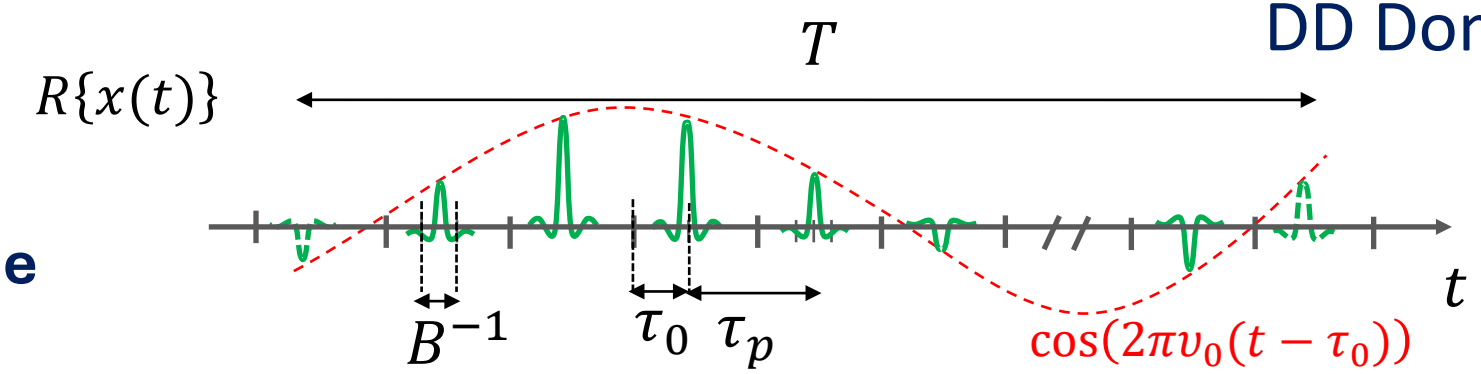

$Z_t^{-1}: \; x_{dd}(\tau,\nu) \rightarrow x(t)$

$x(t) = \sqrt{\tau_p} \int_0^{\nu_p} x_{dd}(t,\nu)\, d\nu$

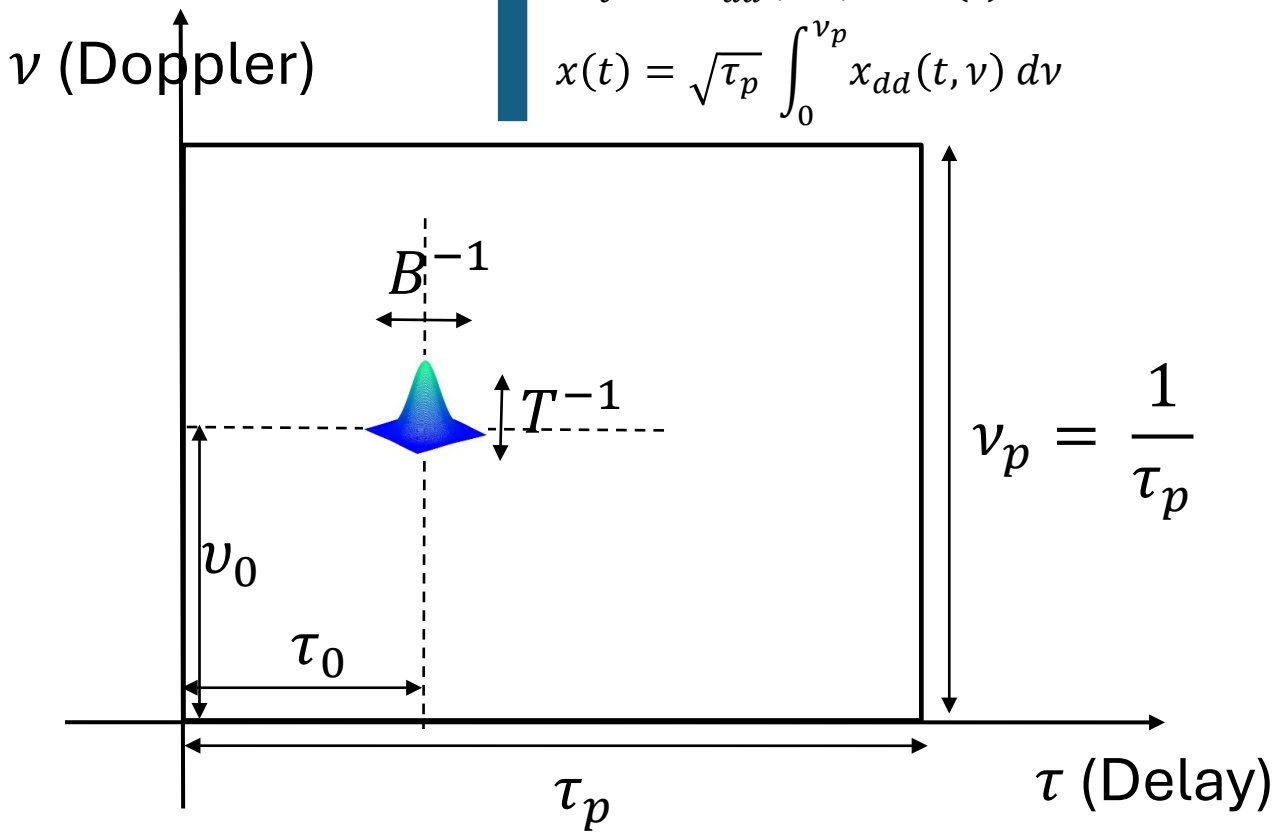

Delay Spread

ν_p= 20 KHz

Doppler Spread

τ_p= 50 μs

Signal Processing in Pictures

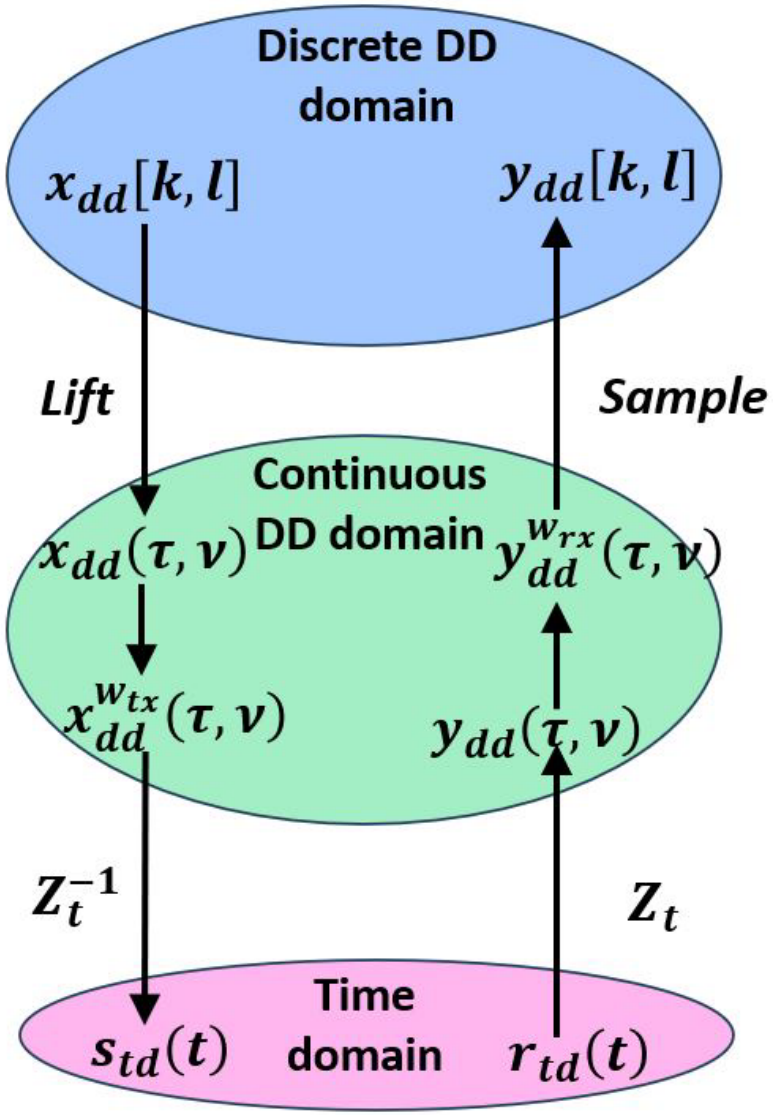

We transmit and receive signals in the time domain

We process signals in the discrete delay-Doppler domain

How to Probe Linear Time-Varying (LTV) Channels

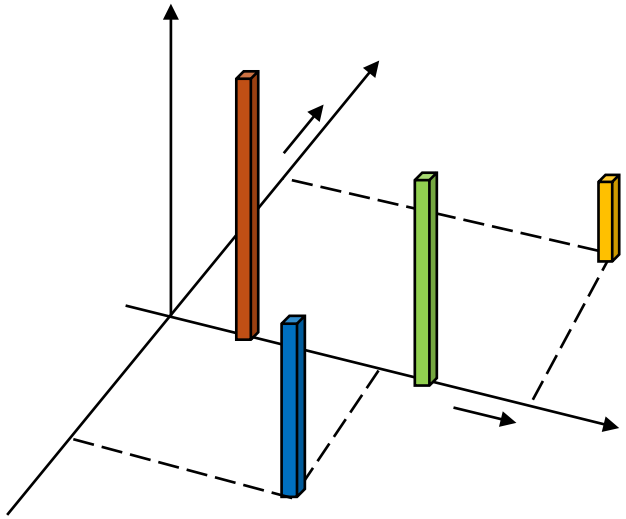

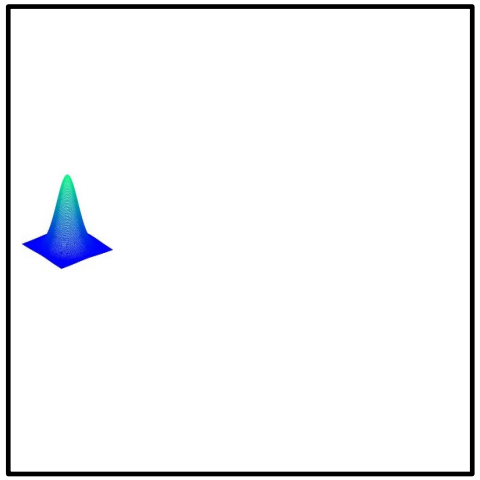

Twisted convolution:

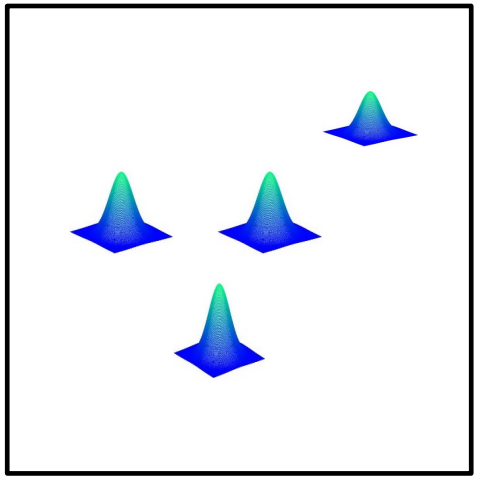

DD Domain Pulse: Geometric mode of an LTV channel

Crystalline Regime: The delay period τ_p is greater than the channel path delay spread, and the Doppler period ν_p is greater than the path Doppler spread:

$$\tau_p > \text{delay spread} \quad \text{and} \quad \nu_p > \text{Doppler spread}$$

$\tau_p \nu_p = 1$: wireless channels are underspread

Signal Bases

$$\boldsymbol{y[n] = \sum_{k,l \in Z_{MN}} h_{eff}[k,l] x[(n-k)_{MN}] \, \xi_{MN}^{l(n-k)} + w[n]}$$

y and x are MN-periodic sequences, $MN = BT$ (time-bandwidth product)

$h_{eff}[k,l]$ captures pulse shaping + physical channel

x can be expanded in terms of an MN-dimensional basis ϕ as:

$$\boldsymbol{x[n] = \sum_{i \in Z_{MN}} s[i] \phi_i[n]}$$

Heisenberg-Weyl Operators

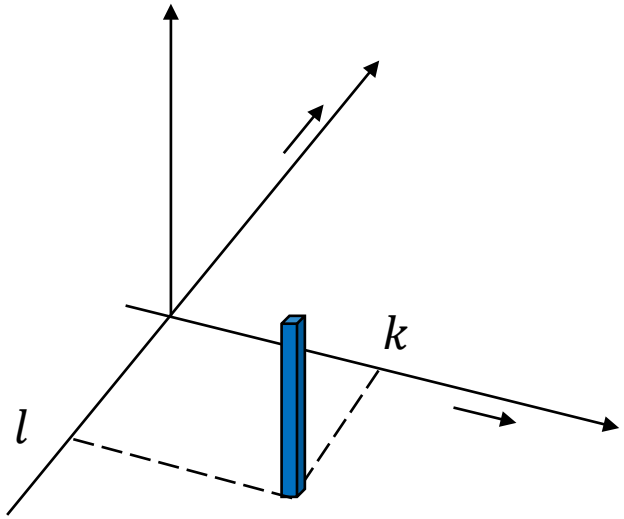

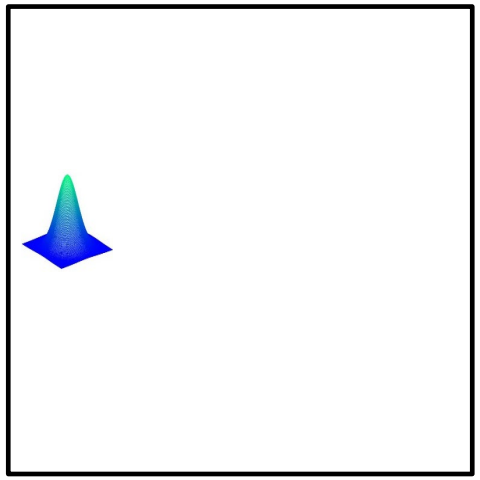

Twisted convolution:

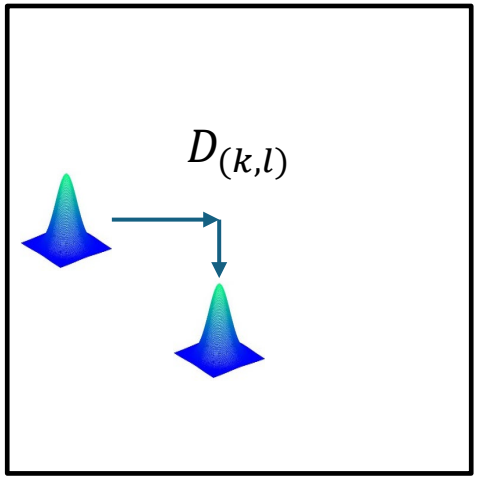

$D_{(k,l)}$ is an operator that shifts an MN-periodic sequence in delay & Doppler

Set of all $D_{(k,l)}$ operators under composition forms the **Heisenberg-Weyl group**:

$$\boldsymbol{H_{MN} = \{\xi_{MN}^{m} D_{(k,l)} | k, l, m \in Z_{MN}\}}$$

Identifying Geometric Modes

There are BT basis elements ϕ_i each spanning a 1-dimensional subspace

$$V_i = \{\xi_{MN}^m \phi_i | m \in Z_{MN}\}$$

The stabilizer of V_i in the Heisenberg-Weyl group is:

$$G_{V_i} = \{\xi_{MN}^m D_{(k,l)} \in H_{MN} | D_{(k,l)}\phi_i = \xi_{MN}^{m'} \phi_i\}$$

The stabilizer G_{V_i} is a maximal commutative subgroup of the Heisenberg-Weyl group

Commutativity follows from the fact that the action on V_i is multiplication by a complex phase

The same maximal commutative subgroup stabilizes all 1-dimensional subspaces V_i

Geometric Modes: common eigenvectors of a maximal commutative subgroup of the Heisenberg – Weyl group

Zak-OTFS Carrier Waveform

Maximal Commutative Subgroup: a rectangular grid T_{MN} in the DD domain

$$\boldsymbol{T_{MN} = \{\xi_{MN}^{m} D_{(aM,bN)} | m \in Z_{MN}, a \in Z_N, b \in Z_M\}}$$

Zak-OTFS carrier waveforms (pulsones): common eigenvectors of T_{MN}

$$\boldsymbol{v_i[n] = \frac{1}{\sqrt{N}} \sum_{d \in Z} \xi_N^{dl_0} \delta[n - k_0 - dM], i = k_0 + l_0 M}$$

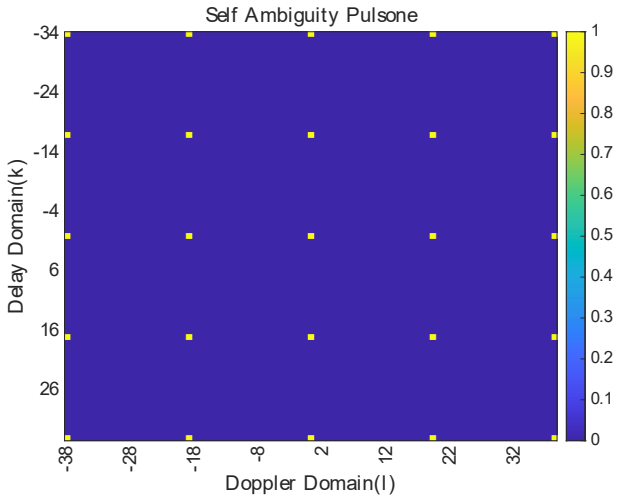

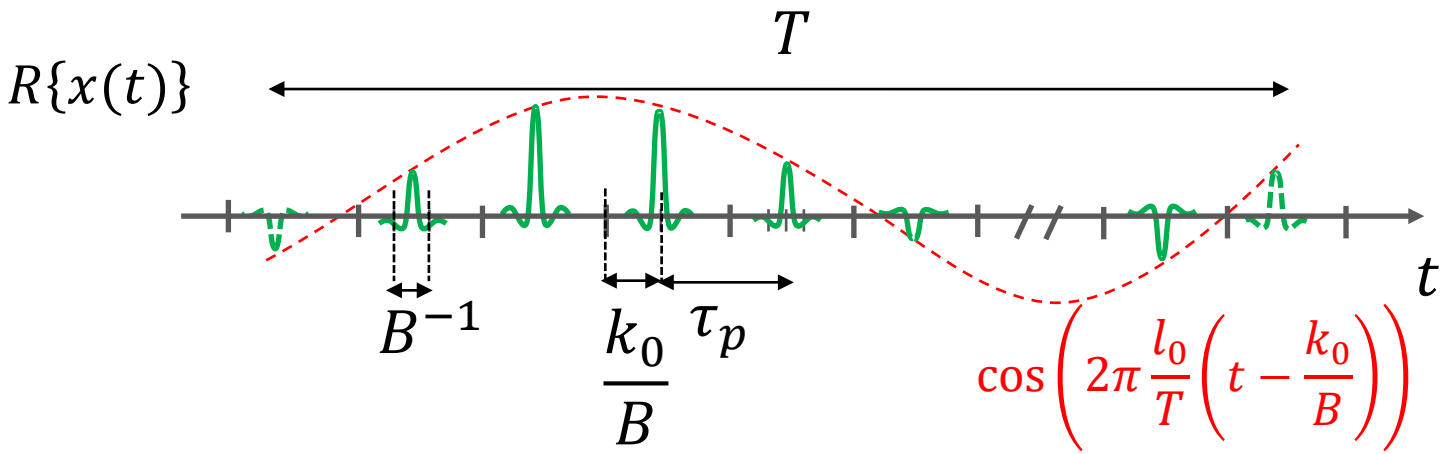

Generalized Discrete Affine Fourier Transform (GDAFT)

GDAFT: Action on an MN-length sequence $x[m]$ is given by:

$$(\boldsymbol{F}_a\boldsymbol{x})[\boldsymbol{n}] = \frac{\mathbf{1}}{\sqrt{\boldsymbol{MN}}} \sum_{\boldsymbol{m=0}}^{\boldsymbol{MN-1}} \boldsymbol{\xi}_{\boldsymbol{MN}}^{\boldsymbol{An^2+Bnm+Cm^2}} \boldsymbol{x}[\boldsymbol{m}]$$

where A, B, C are co-prime to MN

GDAFT is a unitary operator: it preserves inner products & maps bases to bases

GDAFT normalizes $\mathbf{HW_{MN}}$: it is a symplectic transformation

Similar transforms are used in radar signal processing to construct waveform libraries

S.-C. Pei and J.-J. Ding, "Closed-Form Discrete Fractional and Affine Fourier Transforms," IEEE Transactions on Signal Processing, May 2000

GDAFT Maps the Pulsone Basis to a CAZAC Basis

Localized, "peaky"

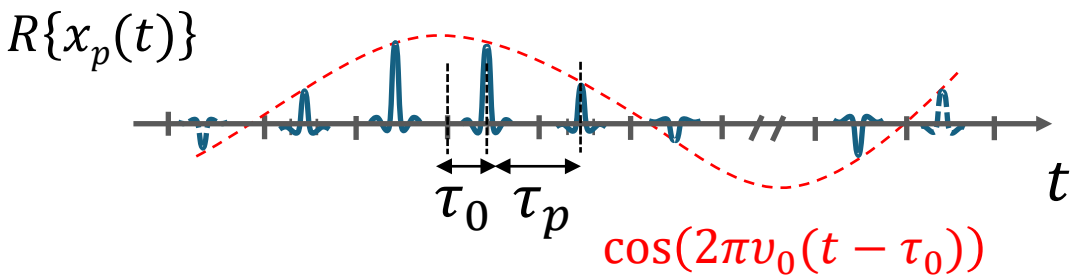

GDAFT

Spread, "noise-like"

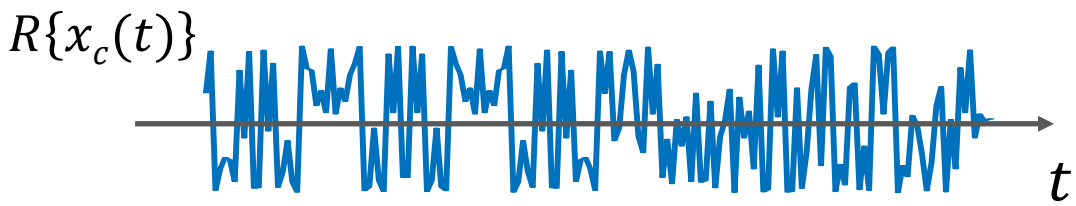

$$\boldsymbol{x_c[n] = (F_a x_p)[n] = \frac{1}{\sqrt{MN}} \xi_{MN}^{un(n+1)/2+kn+\gamma}}$$

CAZAC sequence

with $u = 2(A - (4C)_N^{-1}\, B^2), k = (4C)_N^{-1}(B^2 - 2Bl_0) - A, \gamma = -(k_0 l_0 + (4C)_N^{-1} l_0^2)$

and $k_0 = \frac{M\tau_0}{\tau_p}, l_0 = \frac{N\nu_0}{\nu_p}$

GDAFT Permutes Maximal Commutative Subgroups

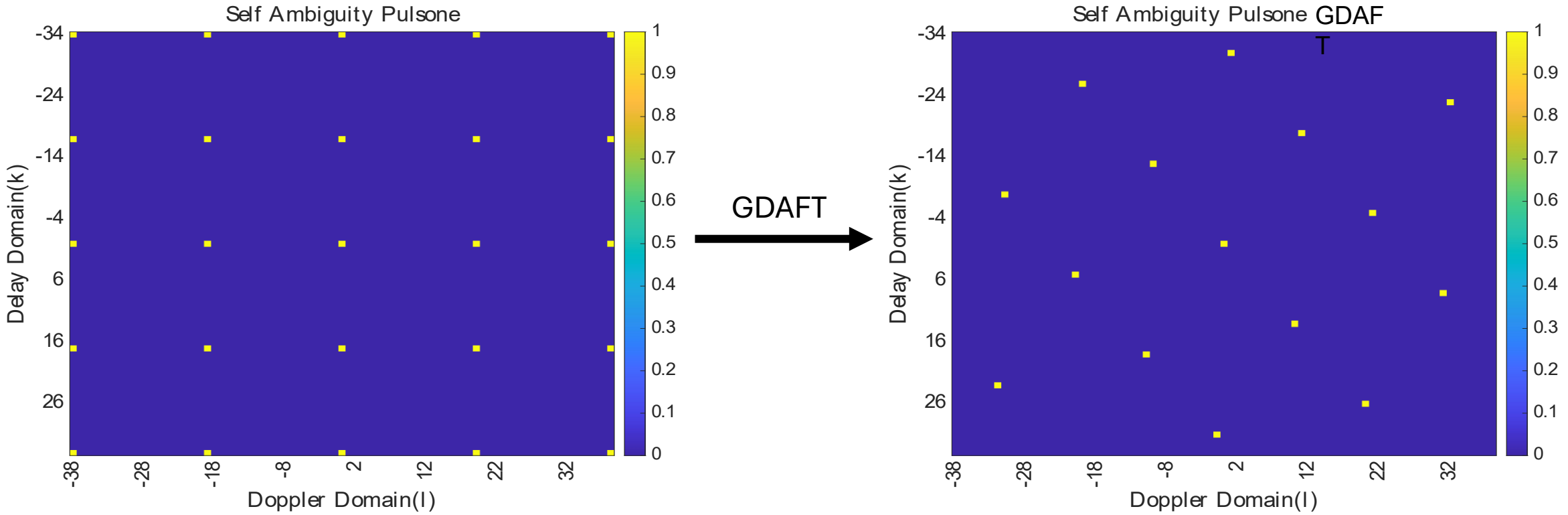

The maximal commutative subgroup is the support of the ambiguity function – rotation of ambiguity functions is central to construction of waveform libraries in radar

D. Cochran et al., "Waveform Libraries," IEEE Signal Processing Magazine, Feb 2009

Ambiguity Function

Consider signals x and y both unit-norm, MN-periodic sequences

Ambiguity Function $A_{y,x}[k,l]$: inner product incorporating correlation in delay and Doppler

$$A_{y,x}[k,l] = \sum_{n \in Z_{MN}} y[n] x^*[(n-k)_{MN}] \, \xi_{MN}^{-l(n-k)}$$

$$x[n] = \sum_{i \in Z_{MN}} s[i] \phi_i[n]$$

Writing x in terms of the basis ϕ gives

$$A_{y,x}[k,l] = \sum_{i \in Z_{MN}} s[i] \underbrace{\sum_{n \in Z_{MN}} y[n] \phi_i^*[(n-k)_{MN}] \, \xi_{MN}^{-l(n-k)}}_{A_{y,\phi_i}[k,l]}$$

If $A_{y,\phi_i}[k,l] = A_{y,\phi_j}[k,l]$ for all $i, j \in Z_{MN}$ then the response at all carriers can be predicted from the response to a single pilot carrier, and the average received power is constant across carriers.

DD Domain Aliasing Controls Predictability

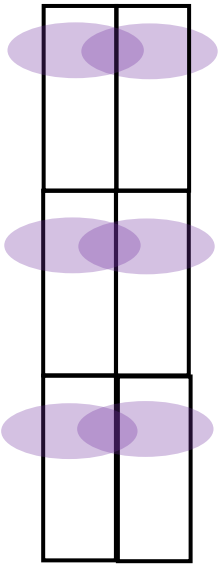

Aliasing in Delay

FDM

$\nu_p \to \infty$

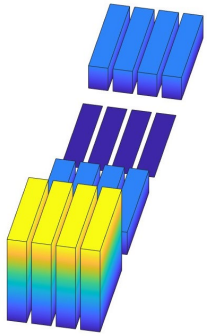

Frequency Selectivity

Predictability

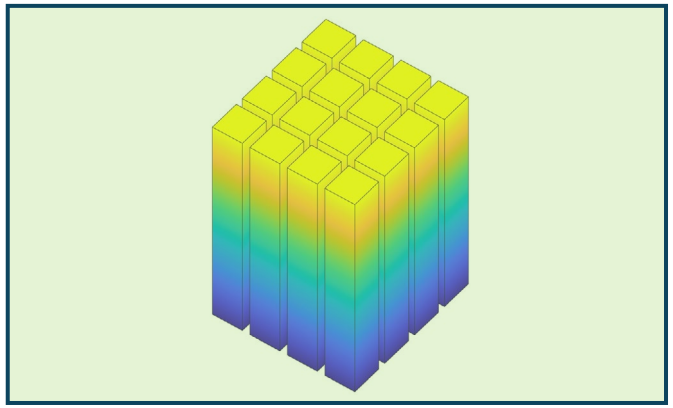

Time Selectivity

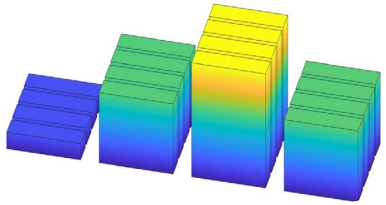

$\tau_p . \nu_p = 1$

TDM

$\tau_p \to \infty$

No Aliasing

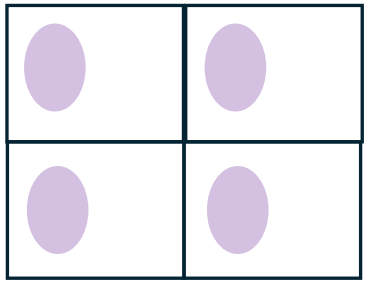

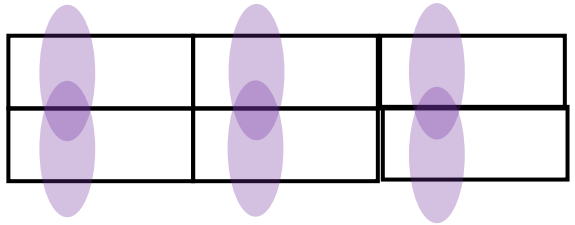

Aliasing in Doppler

Philip Woodward, 1954

Volume under $|A_{s,s}(\tau, \nu)|^2$ fixed by Moyal's Identity but can be redistributed to enable resolution of radar targets

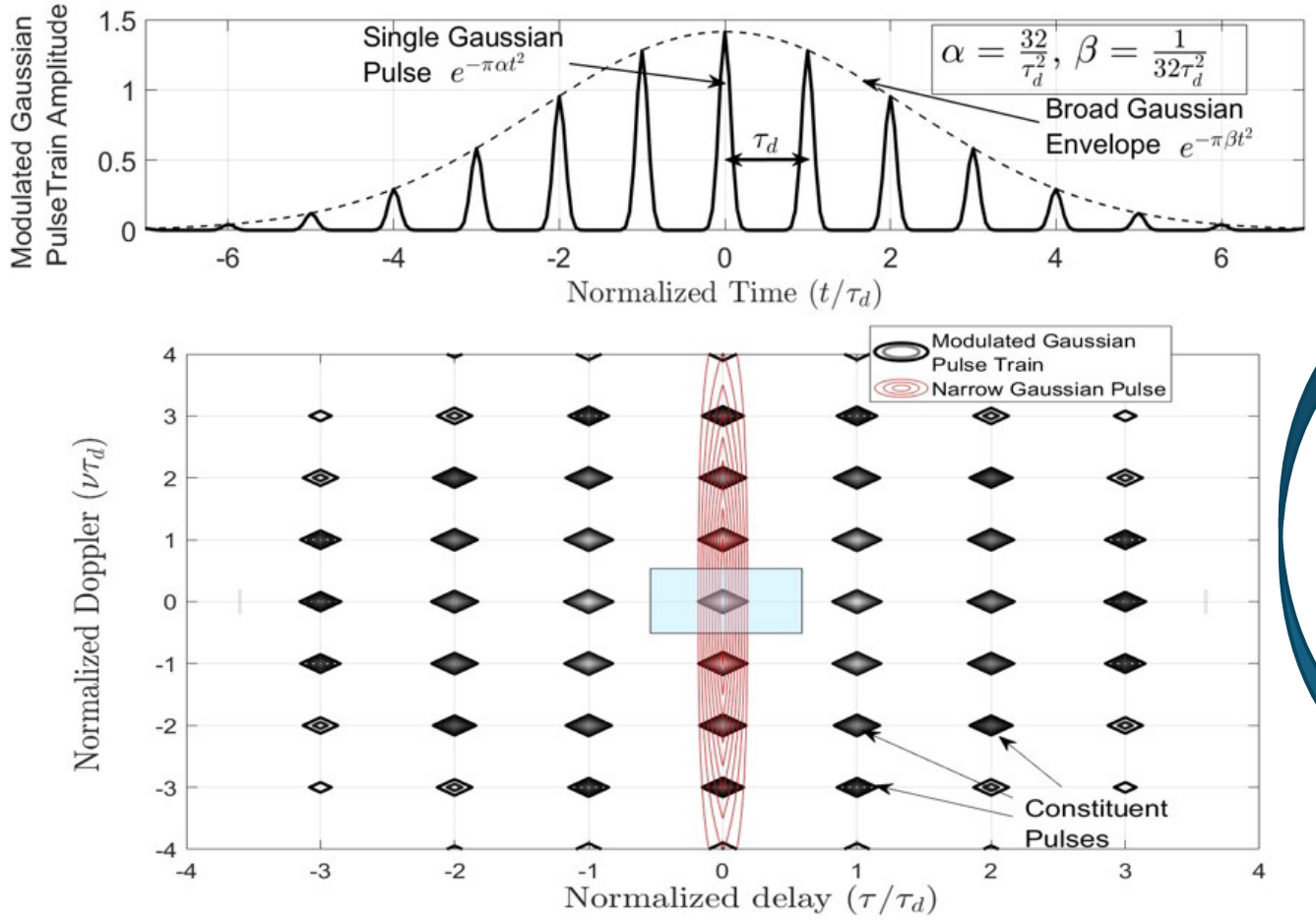

Red Ellipse: Ambiguity function of narrow Gaussian pulse

Modulate a train of narrow TD Gaussian pulses with a broad Gaussian envelope

Black Ellipses

Ambiguity Function $|A_{s.s}(\tau,\nu)|^2$ - pulsone carrier waveform

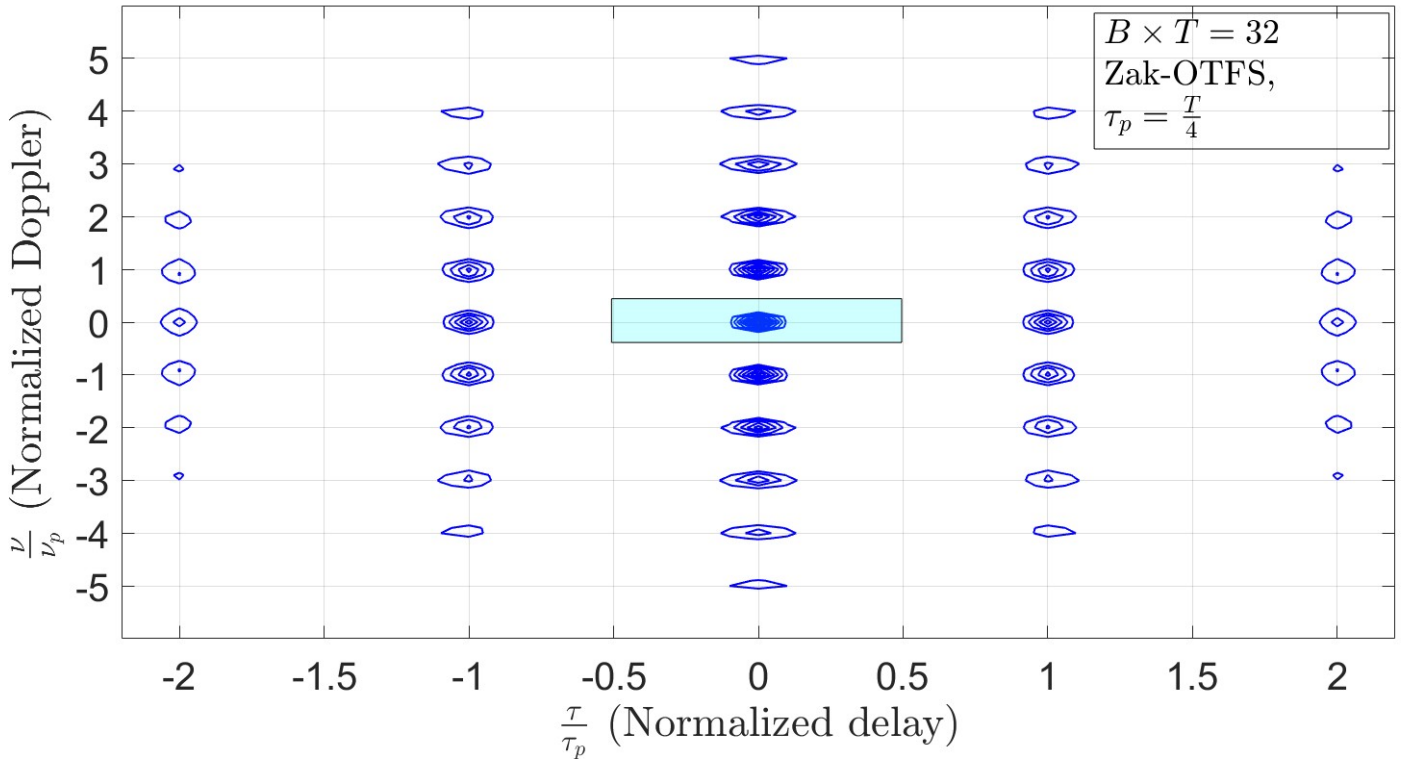

Narrow DD domain impulses separated by τ_p along the delay axis and ν_p along the Doppler axis

Each impulse has a spread of 1/B along the delay axis and 1/T along the Doppler axis

Conclusions

The Heisenberg-Weyl group provides a theoretical foundation for quantum information science and for wireless communication

Quantum bits are eigenvectors of maximal commutative subgroups

Geometric modes of wireless channels are eigenvectors of maximal commutative subgroups

Symplectic transformations change the representation of quantum bits / compute with quantum bits and can be tuned to biased noise

Symplectic transformations change the characteristics of carrier waveforms and rotate ambiguity functions

Supports the perspective of Felix Klein that group theory is applied mathematics